
LOW-RANK INTERCONNECTED ADAPTATION ACROSS LAYERS

Yibo Zhong

Sichuan University
zhongyibo@stu.scu.edu.cn

Yao Zhou

Sichuan University
yaozhou@scu.edu.cn

ABSTRACT

Low-rank adaptation (LoRA) is a powerful parameter-efficient fine-tuning method that utilizes low-rank projectors A and B to learn weight updates ΔW for adaptation targets W . Previous research has shown that LoRA is essentially a gradient compressor, performing random projections on the gradient using a fixed projection matrix A_0 . However, this setup restricts the overall weight update to be low-rank, which limits the adaptation performance. In this paper, we propose low-rank interconnected adaptation across layers (Lily). Specifically, we employ a hierarchical framework where low-dimensional projectors (LPs) retained for downward projection at a particular level, while globally-shared high-dimensional projector (HP) experts perform upward projection across all levels of layers. Lily uniquely connects each LP to all HP experts, therefore the gradient projections are no longer dominated by fixed projection matrices, but rather by selective combinations of all the projectors, thereby breaking the low-rank constraint of LoRA. Furthermore, Lily’s cross-layer connections facilitate the capture of intricate information and dependencies across different layers, thereby enhancing the model’s representational capabilities. Experiments across various modalities, architectures, and model sizes underscore Lily’s great performance and efficiency. Code is available on github <https://github.com/yibozhong/lily>.

1 Introduction

For foundation models like Transformers [Vaswani et al., 2017b], fine-tuning on downstream tasks is a typical usage, but full fine-tuning (FFT) of large models like large language models (LLMs) incurs huge computational and storage costs and risks forgetting previously learned knowledge [Biderman et al., 2024]. Linear probing, which fine-tunes only the final modules like classification heads, addresses these issues but leads to significant performance degradation since it doesn’t update weights from the backbone. To tackle these challenges, parameter-efficient fine-tuning (PEFT) has received significant attention. In PEFT, a model’s backbone weights are frozen, and lightweight trainable modules are introduced to efficiently learn task-specific knowledge. Among all PEFT methods, Low-rank Adaptation (LoRA [Hu et al., 2021]) is one of the most widely applied techniques, especially in LLMs. LoRA introduces a pair of low-rank projection matrices for each adaptation target, consisting of a downward adapter A and an upward adapter B , to approximate ΔW in FFT. Due to its low-rank nature, LoRA offers significant computational and storage savings, effectively alleviating the burdens of FFT while significantly outperforming linear probing by learning the weight updates for backbone weight.

However, LoRA and many subsequent improvements to the method [Miles et al., 2024], [Zhang et al., 2023], [Zhong et al., 2024] have a limitation: the overall learned weight updates ΔW are restricted to be low-rank, which limits the model performance during adaptation. Previous work [Hao et al., 2024] has shown that LoRA adapters are secretly gradient compressors. In particular, LoRA updates to the weight can be approximated by performing random projection on the gradient, using a fixed random projection matrix A_0 , where A_0 is the initial weight for A . Since this limitation arises because the projection matrix is always fixed in LoRA, using multiple distinct matrices and their variations to perform the gradient projection could avoid restricting the weight updates to a low-rank subspace. This prompts a question: *How can we enable high-rank updates by using various projection matrices for an adaptation target?*

In this paper, we propose Low-rank interconnected adaptation across layers (Lily), a novel framework for more expressive and performative PEFT. Specifically, we decouple the downward low-dimensional projector (LP) and its corresponding upward high-dimensional projectors (HP), making them not tightly-bonded. Each LP is connected to

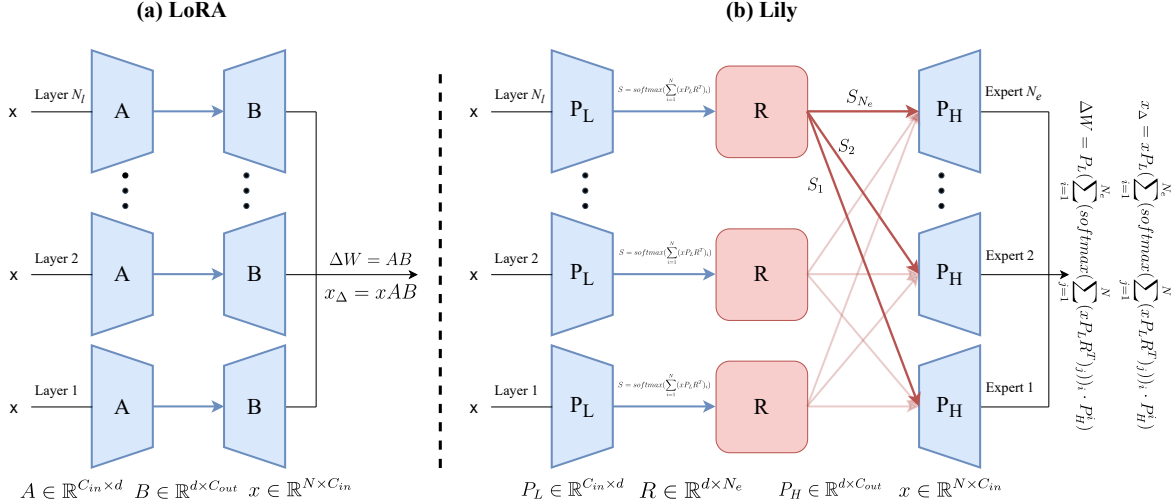


Figure 1: Dynamics of LoRA and Lily. N_l is used to denote the number of layers in the model while N_e denoting the number of high-dimensional projector experts from Lily. R is representing the router from Lily.

all the HPs, and vice versa as shown in Fig. 1. This results in a hierarchical structure where LPs are still retained at a particular level to perform downward projection, while all HPs are now globally shared by all the LPs, performing upward projection. Inspired by self-attention Vaswani et al. [2017a], which calculates the relationship between a token and all tokens and obtains attention scores indicating the strength of their relationship, we selectively connect an LP with the HPs based on layer features. The LP extracts features from the current layer, and based on the extracted features, a data-dependent and selective combination of HPs is performed. This is realized by utilizing a router [Shazeer et al., 2017] that outputs a unique weight distribution for HP experts, depending on the current input feature, thereby exhibiting selectivity.

The gradient projection now uses multiple random projection matrices from all the layers and their selective combinations rather than a fixed matrix, thus effectively avoiding the constraint of low-rank updates from LoRA. Furthermore, Lily enables a more comprehensive information access by allowing adapters at each layer to access information from other layers, promoting an interconnected and dynamic learning process, where the adapters can collaborate, share learned knowledge and model dependencies across layers. Overall, our contributions include:

- We propose Lily, a novel PEFT framework that incorporates cross-layer connections of the projection matrices, thereby breaking the restriction of low-rank weight updates in LoRA.
- Lily utilizes routers to selectively connect an LP with multiple HP experts, enabling comprehensive information access and therefore expressive adaptation.
- Extensive experiments are conducted across various modalities, architectures, and model sizes, highlighting Lily’s great performance and efficiency in diverse scenarios.

2 Related Work

Parameter Efficient Fine-Tuning. Typical usage of foundation models includes pre-training on large datasets and fine-tuning on various downstream tasks. Parameter-efficient fine-tuning (PEFT) thus emerges as a promising field, aiming to fine-tune the model efficiently with minimal parameters while maintaining performance and preserving previously learned knowledge, addressing drawbacks posed by conventional fine-tuning techniques like full fine-tuning or linear probing. Current PEFT research can be mainly categorized into two types: 1) adapter-based methods [Hu et al., 2021], [Chen et al., 2022], [Pfeiffer et al., 2020b], [Jie and Deng, 2023] [Houlsby et al., 2019b] and 2) prompt-based methods [Tu et al., 2023b] [Tu et al., 2023a]. Adapter-based methods introduce lightweight adapters into the Multi-Head Self-Attention (MHSA) or the Feed-Forward Network (FFN) blocks within the Transformer architecture. On the other hand, prompt-based methods append trainable tokens as prompts to the input sequence fed to certain parts of the model.

Among these various PEFT techniques, low-rank adaptation (LoRA [Hu et al., 2021]) stands out as one of the most well-known methods. LoRA introduces a pair of projection matrices A and B per adaptation target W . The low-dimension projector (LP) A projects input x to low-dimension space, and the high-dimension projector (HP) B restores it to its

original dimension. Multiplying these projection matrices approximates the weight update ΔW in FFT. Recent work [Hao et al., 2024] has shown that LoRA adapters are essentially performing random projection to the gradient using a fixed matrix. This restricts the learned weight update to low-rank subspace and thus imitating the model performance. Meanwhile, A and B are tightly coupled, therefore the adaptation process only has information access from current layer, without an understanding of information from other layers, which could be beneficial to modeling dependencies across various layers.

Mixture of Experts. Mixture of Experts (MoE) is an active research area that has garnered significant attention, especially in the field of large language models (LLMs). Conditional computation, where different parts of the network are activated on a per-example basis, has been proposed to enhance model capability without increasing computation [Davis and Arel, 2013] [Bengio et al., 2013] [Eigen et al., 2013] [Almahairi et al., 2016]. The sparsely-gated MoE layer is introduced to implement this idea, consisting of numerous sub-networks [Shazeer et al., 2017]. A trainable gating network, known as a "router", determines the combination of experts for each example. There are already PEFT methods like MoLORA [Zadouri et al., 2023] and MOLA [Gao et al., 2024a] which apply the MoE design concept to PEFT. However, these methods simply treat the adapters combined in LoRA as a single expert. A concurrent research Wu et al. [2024], utilizes LP and HP sub-spaces as the experts but fails to overcome the limitation discussed in previous section.

3 Methodology

3.1 Preliminaries

LoRA is a Gradient Projector. Adaptation process of low-rank adaptation (LoRA) can be expressed as follows when setting the rank to d , a small hidden-dimension:

$$W = W_0 + AB \quad (1)$$

where $W, W_0 \in \mathbb{R}^{C_{in} \times C_{out}}$ with C_{in} being the input dimension and C_{out} being the output dimension. W_0 is the frozen weight of a target module and W is the actual value of the target during adaptation runtime. $A \in \mathbb{R}^{C_{in} \times d}$ and $B \in \mathbb{R}^{d \times C_{out}}$ are low-dimension projectors (LP) and high-dimension projectors (HP), with their product multiplied by a scalar value s (omitted in the equation) to approximate weight update $\Delta W \in \mathbb{R}^{C_{in} \times C_{out}}$. We denote the information from W_0 as the basic knowledge that the pre-trained model already possesses, while $\Delta W = AB$ represents the learned extra knowledge specific to the current downstream task. We denote the initial value of A and B as A_0 and B_0 , and their update as ΔA and ΔB . B_0 is initialized as 0. The approximation is then described as:

$$W = W_0 + (A_0 + \Delta A)(B_0 + \Delta B) \quad (2)$$

$$= W_0 + A_0\Delta B + \Delta A\Delta B \quad (3)$$

$$\approx W_0 + A_0\Delta B \quad (4)$$

It is proved in Hao et al. [2024] that it is the term $A_0\Delta B$ that contributes the most to the weight updates. The forward pass given an input in LoRA is:

$$y = xW = xW_0 + xAB \quad (5)$$

where $x \in \mathbb{R}^{C_{in}}$ and $y \in \mathbb{R}^{C_{out}}$ for simplicity. Therefore, the gradient w.r.t. B is:

$$\frac{\partial \mathcal{L}}{\partial B} = A^T x^T \frac{\partial \mathcal{L}}{\partial y} \quad (6)$$

$$= A^T (\nabla_W \mathcal{L}) \quad (7)$$

where $x^T \frac{\partial \mathcal{L}}{\partial y} \in \mathbb{R}^{C_{in} \times C_{out}}$ is the gradient for the weight matrix, which we denote as $(\nabla_W \mathcal{L})$. Using the approximation in Eq. 2, we can express the adaptation when only updating B using gradient descent:

$$W = W_0 - \eta \sum_{t=0}^T [A_0 A_0^T (\nabla_W \mathcal{L}_t)] \quad (8)$$

where T is the current time-step and η is the adopted learning rate. The projection matrix here is A_0 because A is not updated in the approximation, since its change contribute little to the overall weight updates. We can observe that LoRA is essentially performing random projection to the gradient using a fixed random projection matrix A_0 . However, this setup limit the weight update ΔW to be low-rank, which also limit the adaptation performance.

Lily is a Better Gradient Projector. Consider simply connecting each A with all the B s with weights, the forward pass is then:

$$W = W_0 + \sum_{i=1}^{N_e} \left[S_i [(A_0 + \Delta A)(B_0^i + \Delta B^i)] \right] \quad (9)$$

$$= W_0 + \sum_{i=1}^{N_e} [S_i (A_0 \Delta B^i + \Delta A \Delta B^i)] \quad (10)$$

$$\approx W_0 + A_0 \sum_{i=1}^{N_e} S_i \Delta B^i \quad (11)$$

where N_e is used to denote the number of B s in the model and S is a set of weight scores of current A for all the B s, each S_i is a scalar value representing the weight for corresponding B^i .

Thanks to the inter-connectivity, each B is also connected to all the A s. The gradient w.r.t an B is now:

$$\frac{\partial \mathcal{L}}{\partial B} = \sum_{i=1}^{N_l} C_i A^{iT} x^{iT} \frac{\partial \mathcal{L}}{\partial y^i} \quad (12)$$

$$= \sum_{i=1}^{N_l} C_i A^{iT} (\nabla_{W_i} \mathcal{L}) \quad (13)$$

where N_l is the number of A s in the model and we denote gradient for each corresponding weight matrix as $\nabla_{W_i} \mathcal{L}$. C is a set of weight scores where each C_i is a weight score from certain A_i for current B . The forward pass when only updating B can then be expressed as:

$$W = W_0 - \eta \sum_{t=0}^T \left[\sum_1^{N_e} S_i \left[\sum_{j=1}^{N_l} C_{i,j} A_0 A_0^j T (\nabla_{W_j} \mathcal{L}_t) \right] \right] \quad (14)$$

where $C_{i,j}$ is used to denote weight scores from various $A^j, j \in \{1, 2, \dots, N_l\}$ to $B_i, i \in \{1, 2, \dots, N_e\}$. It can be observed that with this setup, the projection to the gradient no longer use a fixed A_0 , but rather utilizing all the projection matrix $A_0^i, i \in \{1, 2, \dots, N_l\}$ and their overall complex combinations. Note that all the A_0^i s are distinct random projection matrices and each weight score (S_i and $C_{i,j}$) is unique, data-dependent and thus varies across time-steps. Therefore, the weight updates are not restricted to be low-rank, but rather high-rank. **This setup is precisely what Lily adopts.** To differentiate from LoRA, we use different notations for the projectors. Specifically, we decouple HPs from their original layers, allowing them to form a model-wide shared module of HP experts (B in LoRA), denoted as P_H^i , where $i \in \{1, 2, \dots, N_e\}$ and N_e is the number of HP experts. Meanwhile, we fix LPs (A in LoRA) $P_L^i, i \in \{1, 2, \dots, N_l\}$ in each layer for downward projection, where N_l is the number of LPs. This hierarchical structure makes the projection matrices all interconnected across layers, enabling the modeling of complex dependencies and high-rank updates to the model weights. Detailed model structure and design intuitions are discussed in Appendix A.

3.2 Dynamics of Lily

Downward Projection and Selective Weight Allocation. The process is illustrated in the right half of Fig. 1. Initially, we use an LP to project the input $x \in \mathbb{R}^{N \times C_{in}}$ into its low-dimensional representation $x' \in \mathbb{R}^{N \times d}$ where N is the sequence length:

$$x' = x P_L \quad (15)$$

Inspired by the Mixture of Experts (MoE) paradigm, we employ a router $R \in \mathbb{R}^{N_e \times d}$ to selectively assign weights to all HP experts based on their relationship to the current layer's features (x'). The weight set S is obtained as:

$$S = \text{softmax} \left(\sum_{i=1}^N (x' R^T)_i \right) \quad (16)$$

The router selectively combines experts based on the current layer's features, enabling smart information integration. For shallower inputs, the router increases attention for experts specializing in shallow-layer knowledge, while deeper inputs favor experts learning deep-layer knowledge.

Table 1: Commonsense reasoning results for Falcon-Mamba-7B across eight tasks. Bold represents the highest performance for each dataset utilizing PEFT methods.

Model	PEFT	BoolQ	PIQA	SIQA	HellaSwag	WinoGrande	ARC-e	ARC-c	OBQA	Avg.
ChatGPT	-	73.1	85.4	68.5	78.5	66.1	89.8	79.9	74.8	77.0
Falcon-Mamba-7B	LoRA	6.5	30.5	40.6	14.9	56.4	42.2	31.8	38.4	32.7
	Lily (Δ + in)	44.9	66.8	65.0	10.5	57.1	78.7	64.6	68.2	57.0
	Lily (in)	60.2	61.0	67.3	12.9	61.5	80.0	67.5	65.8	59.5

Table 2: Commonsense reasoning results for LLaMA3-8B across eight tasks. [†] represents results taken from Liu et al. [2024]. Bold denotes the highest performance scores for each dataset among different PEFT methods.

Model	PEFT	BoolQ	PIQA	SIQA	HellaSwag	WinoGrande	ARC-e	ARC-c	OBQA	Avg.
ChatGPT	-	73.1	85.4	68.5	78.5	66.1	89.8	79.9	74.8	77.0
LLaMA3-8B	LoRA [†]	70.8	85.2	79.9	91.7	84.3	84.2	71.2	79.0	80.8
	PiSSA	67.1	81.1	77.2	83.6	78.9	77.7	63.2	74.6	75.4
	MiLoRA	68.8	86.7	77.2	92.9	85.6	86.8	75.5	81.8	81.9
	Lily	72.9	85.6	77.8	92.7	83.3	89.7	77.6	82.8	82.8

Weighted Combination of Experts and Upward Projection. Once we obtain the low-dimensional input x' , we combine information from all layers using the model-wide shared global HP module. One intuitive approach is to feed x' into each HP expert and combine their outputs to obtain the extra knowledge $x_{\Delta} \in \mathbb{R}^{N \times C_{out}}$:

$$x_{\Delta} = \sum_{i=1}^{N_e} S_i \cdot (x' P_H^i) \quad (17)$$

where $S \in \mathbb{R}^{N_e}$ is the set of weight scores for HP experts, obtained through selective weight allocation. To address efficiency concerns discussed in Appendix A.2, we propose an alternative implementation that is mathematically equivalent and significantly reduces computational burden, described as:

$$x_{\Delta} = x' \left(\sum_{i=1}^{N_e} S_i \cdot P_H^i \right) \quad (18)$$

Since each S_i is a scalar value, the calculation in Eq. 18 is mathematically equivalent to that in Eq. 17, but with significantly improved efficiency. Therefore, the whole computation flow, with input $x \in \mathbb{R}^{N \times C_{in}}$ and output $y \in \mathbb{R}^{N \times C_{out}}$, for an adaptation target module is:

$$y = xW_0 + s \cdot x_{\Delta} \quad (19)$$

$$= xW_0 + s \cdot xP_L \left(\sum_{i=1}^{N_e} \left(\text{softmax} \left(\sum_{j=1}^N (xP_L R^T)_j \right) \right)_i \cdot P_H^i \right) \quad (20)$$

By selectively allocating weights and combining HP experts, Lily enables access to all levels of information during adaptation. Each layer’s target adaptation modules could consider the status and knowledge from all other layers, resulting in a more expressive and comprehensive adaptation. Meanwhile, thanks to its inter-connectivity and selectivity, Lily break the low-rank update constraint of LoRA and enable high-rank updates, as discussed in preliminaries.

4 Experiments

We validate the effectiveness of Lily across different domains, model sizes (from ViT to LLM), and architectures (Transformers, Mamba), demonstrating its general strong adaptation capability. Concurrently, we conduct a comprehensive analysis of Lily’s intrinsic mechanisms, providing a thorough understanding of Lily. All experiments are conducted on a single RTX 4090 GPU. Additionally, multiple analysis are provided in Appendix C, D, E, F, G, H, I and J.

4.1 Common Sense Reasoning

Implementation We evaluate Lily on commonsense reasoning with LLMs. Regarding the implementation, we utilize LLaMA3-8B [AI@Meta, 2024] and Falcon-Mamba-7B [Zuo et al., 2024] as backbones. LLaMA3 is a near-SOTA

Table 3: Various fine-tuning methods applied to RoBERTa Base are evaluated on 6 datasets from the GLUE benchmark. We present the Matthew’s correlation coefficient (MCC) for CoLA, Pearson correlation coefficient (PCC) for STS-B, and accuracy (Acc.) for the remaining tasks. The highest performance for each dataset is highlighted in **bold**, with all metrics favoring higher values across the 6 datasets.

Model & Method	# Trainable Parameters	SST-2 (Acc.)	MRPC (Acc.)	CoLA (MCC)	QNLI (Acc.)	RTE (Acc.)	STS-B (PCC)	Avg.
RoB _{base} (FFT)	125M	94.8	90.2	63.6	92.8	78.7	91.2	85.2
RoB _{base} (BitFit)	0.1M	93.7	92.7	62	91.8	81.5	90.8	85.4
RoB _{base} (Adpt ^D)	0.3M	94.2	88.5	60.8	93.1	71.5	89.7	83.0
RoB _{base} (Adpt ^D)	0.9M	94.7	88.4	62.6	93.0	75.9	90.3	84.2
RoB _{base} (LoRA)	0.3M	95.1	89.7	63.4	93.3	78.4	91.5	85.2
RoB _{base} (AdaLoRA)	0.3M	94.5	88.7	62.0	93.1	81.0	90.5	85.0
RoB _{base} (DyLoRA)	0.3M	94.3	89.5	61.1	92.2	78.7	91.1	84.5
RoB _{base} (Lily)	0.3M	95.0	90.2	66.0	92.5	81.6	90.8	86.0

open-source large language model, while Falcon-Mamba is the latest and only open-source large language model based on the Mamba architecture. Using these models allows us to validate the effectiveness of Lily for fine-tuning LLMs and whether this effectiveness can be transferred to architectures beyond Transformers (Mamba, in this case). We fine-tune these models on Commonsense170K [Hu et al., 2023] and evaluate the adaptation results on eight multiple-choice problem tasks, including BoolQ [Clark et al., 2019], PIQA [Bisk et al., 2020], SIQA [Sap et al., 2019], HellaSwag [Zellers et al., 2019], WinoGrande [Sakaguchi et al., 2021], ARC-e, ARC-c [Clark et al., 2018], and OBQA [Mihaylov et al., 2018]. The compared methods are LoRA for Falcon-Mamba and LoRA [Hu et al., 2021], PiSSA [Meng et al., 2024], and MiLoRA [Wang et al., 2024] for LLaMA3. We only compare LoRA for Falcon-Mamba because tailored PEFT methods for Mamba-based LLMs have not yet been proposed, which is beyond the scope of this paper. Detailed hyper-parameter settings and datasets information are reported in Appendix B.1.1 and Appendix B.2.1.

Results We report the accuracy in the Table 2 and Table 1. Based on the results, it is evident that Lily performs the best out of the compared PEFT methods. Lily surpasses LoRA by a significant margin on Falcon-Mamba, and on LLaMA3, it outperforms LoRA and MiLoRA. This indicates Lily’s superior adaptation capability and parameter efficiency dealing with commonsense reasoning tasks. Additionally, while the performance on Falcon-Mamba is notably lower than the baseline and LLaMA3, we believe this is due to the model’s limitations rather than Lily’s, as Lily still significantly outperforms LoRA on Falcon-Mamba and demonstrates great performance on LLaMA3. This sheds light on the current state of Mamba-based LLMs, showing that they generally have inferior performance compared to Transformer-based LLMs like ChatGPT and LLaMA on many tasks.

4.2 Natural Language Understanding

Implementation We evaluate Lily on natural language understanding (NLU) tasks. For implementation, we use RoBERTa Base [Liu et al., 2019] as the backbone and fine-tune it on tasks from GLUE benchmark (General Language Understanding Evaluation [Wang et al., 2018]), consisting of multiple NLU tasks including single-sentence classification tasks, similarity and paraphrase tasks and natural language inference tasks. We compare Lily against several competitive PEFT methods, including BitFit [Zaken et al., 2021], Adapter-Tuning [Rücklé et al., 2020] [Houlsby et al., 2019a] [Lin et al., 2020] [Pfeiffer et al., 2020a], LoRA [Hu et al., 2021], DyLoRA [Valipour et al., 2022] and AdaLoRA [Zhang et al., 2023]. Additionally, we utilize full fine-tuning (FFT) as the baseline. Specific hyper-parameters and datasets information are provide in Appendix B.1.2 and B.2.2.

Results The results are shown in Table. 3, from which we can clearly observe that Lily surpass all of the compared PEFT methods by a significant margin, demonstrating its capability of tackling NLU tasks. Among the 6 given tasks, Lily surpasses FFT in 4 of them, showcasing its strong approximation ability with compatible parameter-efficiency.

4.3 Subject-driven Image Generation

Implementation We conduct experiments on fine-tuning text-to-image diffusion models for the subject-driven generation task [Ruiz et al., 2023]. For backbone, we use SDXL and we fine-tune it using LoRA and Lily. We first fine-tune

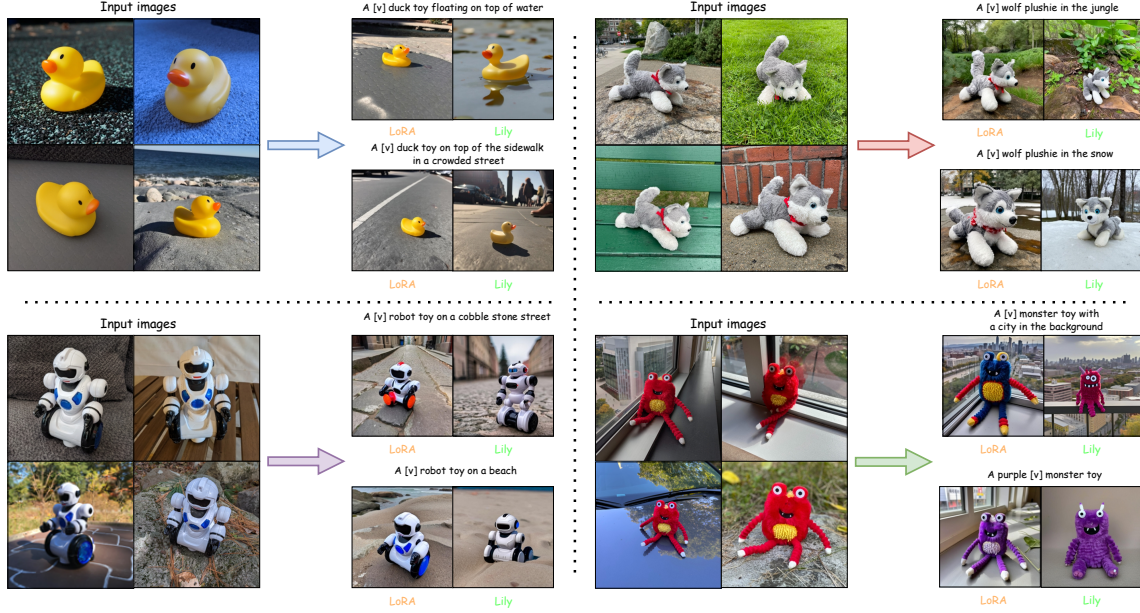


Figure 2: Results of subject-driven generation. Lily’s results align better with prompts, featuring more accurate color, environment, and shape.

Table 4: Full results of Lily on ViT-B pre-trained on ImageNet-21K for the VTAB-1K benchmark, with averages computed based on group-wise results. **Bold** indicates the best performance.

			Natural							Specialized				Structured							
	Params(M)	Average	Cifar100	Caltech101	DTD	Flowers102	Pets	SVHN	Sun397	Camelyon	EuroSAT	Resisc45	Retinopathy	Clevr-Count	Clevr-Dist	DMLab	KITTI-Dist	dSpr-Loc	dSpr-Ori	sNORB-Azim	sNORB-Ele
<i>Conventional Fine-Tuning</i>																					
FFT	86	68.9	68.9	87.7	64.3	97.2	86.9	87.4	38.8	79.7	95.7	84.2	73.9	56.3	58.6	41.7	65.5	57.5	46.7	25.7	29.1
LP	0	57.6	64.4	85.0	63.2	97.0	86.3	36.6	51.0	78.5	87.5	68.5	74.0	34.3	30.6	33.2	55.4	12.5	20.0	9.6	19.2
<i>PEFT methods</i>																					
AdaptFormer	0.588	76.8	74.0	92.2	71.7	99.3	91.7	88.9	56.4	87.2	95.1	85.7	75.9	84.2	62.2	53.0	81.0	87.1	53.6	35.3	42.3
Bi-LoRA	1.180	76.7	72.1	91.7	71.2	99.1	91.4	90.2	55.8	87.0	95.4	85.5	75.5	83.1	64.1	52.2	81.3	86.4	53.5	36.7	44.4
LoRA	1.180	76.4	72.5	91.5	71.9	99.1	91.4	89.6	56.0	87.6	95.3	84.0	75.0	83.6	64.3	51.6	80.9	86.0	51.8	36.8	42.3
FourierFT	0.936	72.7	69.1	88.8	71.9	99.0	91.0	79.0	55.6	84.9	93.0	83.2	74.9	70.7	61.1	45.2	74.8	78.0	53.0	24.8	30.8
MoRA	1.058	75.4	72.1	90.0	71.7	99.2	91.1	90.1	56.0	87.1	94.8	85.1	75.4	76.7	62.3	49.7	78.3	83.1	53.0	34.5	34.5
Lily	0.318	77.3	73.9	93.0	72.9	99.3	91.6	89.0	56.6	87.9	95.2	84.9	75.7	83.9	65.4	53.4	81.6	88.2	54.5	37.0	45.4

the model with images associated with text prompts (e.g., A photo of a [v] duck toy), in which a unique identifier is provided. After that, text prompts containing the identifier could be used to generate customized images.

Results The results are presented in Fig. 2 following the format in Gao et al. [2024b] and Wu et al. [2024], from which we can observe that images generated by Lily generally align better with the text prompts. For instance, when asked to generate a duck toy floating on top of water, Lily’s image accurately depicts the designated environment, whereas LoRA’s does not. Additionally, when asked to generate a wolf plushie in snow, Lily precisely depicts the snow around the wolf, while LoRA fails to do so. These observations demonstrate Lily’s excellent ability in the domain of text-to-image generation with more expressive adaptation. More generated results are in Appendix I.

4.4 Visual Adaptation Benchmark

Implementation We assess Lily on the Visual Task Adaptation Benchmark (VTAB-1K Zhai et al. [2019]), a suite of 19 visual tasks spanning diverse domains and semantics, to test its general visual adaptation capability. Tasks are

Table 5: Full results of Lily on Vim-S pre-trained on ImageNet-1K for the VTAB-1K benchmark, with averages calculated within each group. * denotes linear probing results from [Tu et al. \[2023b\]](#). For fair comparison, we also use ViT-B pre-trained on ImageNet-1K. **Bold** indicates best performance among Vim-based PEFT methods.

		Params(M)	Average	Natural						Specialized				Structured							
				Cifar100	Caltech101	DTD	Flowers102	Pets	SVHN	Sun397	Camelyon	EuroSAT	Resisc45	Retinopathy	Clevr-Count	Clevr-Dist	DMLab	KITTI-Dist	dSpr-Loc	dSpr-Ori	sNORB-Azim
Conventional Fine-Tuning																					
FFT-Vim	26	70.1	47.7	89.4	64.2	89.0	87.7	90.6	35.1	84.5	93.9	81.0	74.5	67.5	52.9	47.3	78.9	75.3	53.9	33.3	29.4
FFT-ViT	86	69.9	49.4	89.3	65.5	91.7	89.1	91.4	33.5	85.9	93.6	85.4	74.3	54.7	55.2	48.7	79.7	68.2	49.7	31.5	27.7
LP-Vim	0	55.3	40.9	83.3	57.3	66.3	86.3	38.4	34.6	79.0	87.6	65.0	73.6	36.3	35.1	33.3	64.8	23.0	21.6	15.1	21.7
LP-ViT	0	66.4	50.6	85.6	61.4	79.5	86.5	40.8	38.0	79.7	91.5	71.7	65.5	41.4	34.4	34.1	55.4	18.1	26.4	16.5	24.8
PEFT on ViT																					
AdaptFormer	0.147	72.4	56.2	89.6	67.2	91.2	91.1	85.9	42.1	85.4	94.6	84.0	74.3	75.8	58.6	48.6	79.6	81.6	53.7	29.6	35.2
LoRA	0.295	72.5	56.4	89.0	66.9	91.2	90.4	86.9	41.5	85.4	95.1	84.1	75.2	75.8	61.7	47.7	80.5	80.4	52.0	29.4	35.7
PEFT on Vim																					
LoRA	0.054	70.1	57.5	87.7	64.4	86.0	90.0	85.7	39.8	82.2	93.8	79.6	72.5	78.6	56.5	42.0	80.5	71.8	51.0	28.4	32.6
Lily-S	0.074	71.4	58.2	88.5	65.6	87.1	90.7	87.5	40.4	83.3	94.1	79.7	73.8	81.2	57.3	44.1	80.9	79.3	54.1	30.0	33.7
Lily-L	0.196	72.3	57.8	89.4	66.2	87.8	90.5	88.1	40.5	84.1	94.3	81.3	75.1	81.6	57.8	46.5	81.0	82.9	55.2	32.1	34.8

categorized into Natural, Specialized, and Structured, all formulated as classification problems for consistent model evaluation. We conduct two sets of experiments: one focusing on the adaptation effectiveness on Vision Transformer (ViT [[Dosovitskiy et al., 2020](#)]) and the other on Vision Mamba (Vim [[Zhu et al., 2024](#)]), demonstrating Lily’s architecture-agnostic capabilities. For ViT, we use ViT-B pre-trained on ImageNet-21K [[Deng et al., 2009](#)], and for Vim, Vim-s pre-trained on ImageNet-1K. To fairly compare ViT and Vim architectures, we implement LoRA [[Hu et al., 2021](#)] and AdaptFormer [[Chen et al., 2022](#)] on ViT-B pre-trained on ImageNet-1K. In ViT experiments, we compare Lily with LoRA, AdaptFormer, FourierFT [[Gao et al., 2024b](#)], and MoRA [[Jiang et al., 2024](#)]; in Vim experiments, we focus on contrasting architectures difference, therefore only using LoRA as the baseline. All experiments include FFT and linear probing as baselines. For Vim, we implement two versions: Lily-S (Small) and Lily-L (Large) of Lily, with different hyperparameter settings to either reduce the parameter count (Lily-S) or maximize performance (Lily-L). For Lily on ViT, the reported results are obtained from adapting both the self attention and the MLP module in Transformer. For the performance w.r.t the fine-tuned module, we conduct additional experiments in Appendix D. Detailed experimental settings and datasets information are provide in Appendix B.1.3 and B.2.3.

Results Results are shown in Table 4 and Table 5. For ViT, Lily significantly outperforms all compared PEFT methods with improved parameter efficiency. For Vim, results on ViT generally surpass those on Vim. For instance, LoRA on ViT performs better than LoRA on Vim. We argue that this is due to differences in architecture designs and general model sizes. However, Lily’s strong adaptation performance allows it to match or exceed PEFT methods on ViT and significantly outperform LoRA on Vim (Lily-S and Lily-L surpass LoRA by a significant margin). This demonstrates Lily’s architecture-agnostic capability, highlighting its potential across various model architectures. In general, Lily has achieved great visual adaptation capability with an advantage of being architecture-agnostic and enjoying excellent parameter-efficiency.

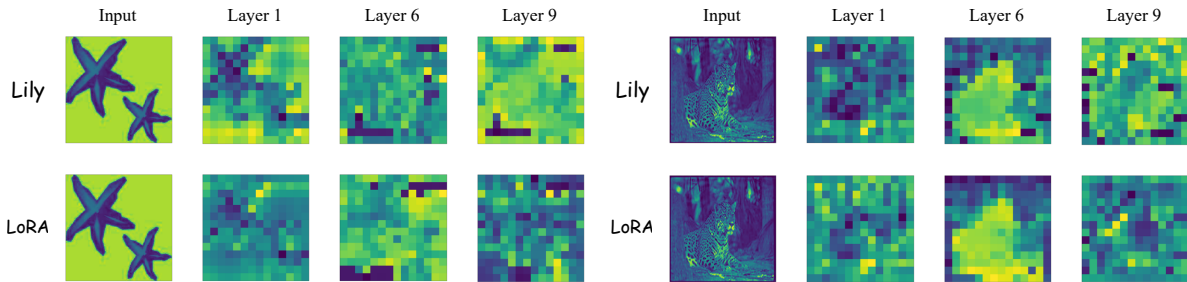


Figure 3: Attention maps of Lily and LoRA. The input images for the example here are taken from Caltech101 datasets from VTAB-1K benchmark. It can be observed that features from a certain layer have more similarity to those in other layers in Lily than in LoRA.

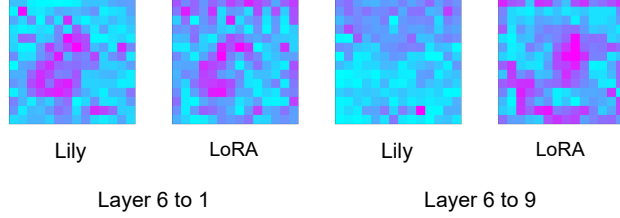


Figure 4: Feature difference measured in absolute distance for each element. We compare Lily and LoRA in terms of the difference between features from different layers. In this example image taken from Caltech101, we visualize the feature difference between layers 6 and 1, as well as between layers 6 and 9.

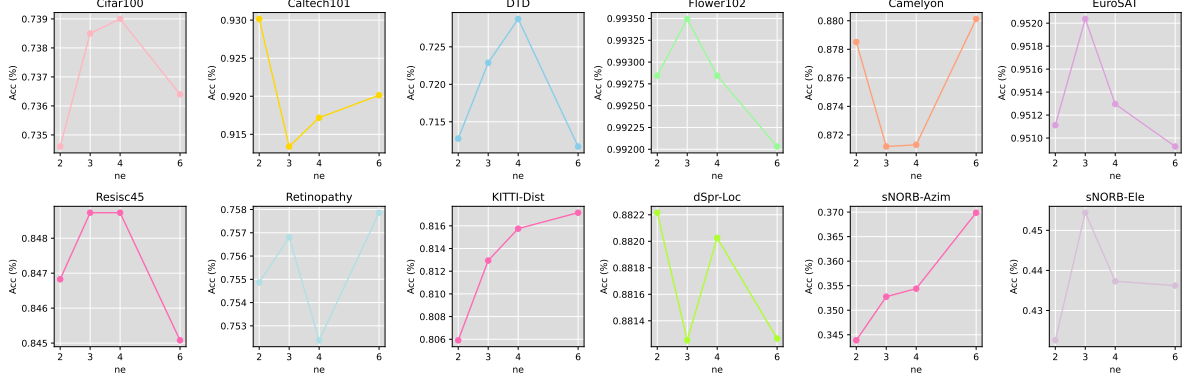


Figure 5: Impact of attention granularity (i.e., the choice of how many LPs and HPs) on the performance. We choose 12 out of 19 tasks from VTAB-1K for a comprehensive understanding.

4.5 Understanding Lily

From a Feature Merging Perspective. Apart from being a better gradient projector than LoRA, Lily also enables comprehensive information access across layers. Lily enables access to information or features from all other layers when adapting a target module at a specific layer thanks to the inter-connectivity of the adapters. We aim to understand how Lily achieves this comprehensive information access from the perspective of visual tasks as shown in Fig. 3. We can observe that, in Lily, the distinctness of the attention maps between layers is not as pronounced as in LoRA. This validates Lily’s ability to enable all-level information access, since adaptation at each layer takes into account features from other layers. Additionally, we specifically visualize the actual feature differences between different layers in Fig. 4. We observe that Lily has more points with low feature differences (blue color) than LoRA, indicating that the distinctness of features between layers in Lily is generally lower than in LoRA. This further demonstrates Lily’s ability to enable comprehensive information access. Although we enable all-level information access, what prevents the features from becoming completely identical is the selectivity introduced by Lily, which we specify in the following section.

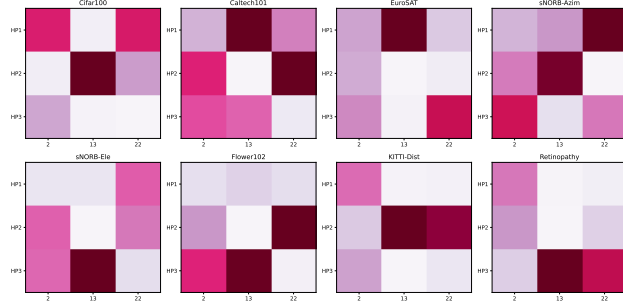


Figure 6: Visualization of accumulated assigned weight for HP experts by a router across various layers. Example here uses layer of index 2, 13 and 22 to represent shallow, middle and deep layers.

What’s the Influence of Attention Granularity? The number of experts in the model-wide HP module can be freely set, and the number of LPs can also be flexibly set by sharing across the same level of layers introduced in Appendix A.1. Therefore, we analyze the impact of these choices on performance. We denote the number of LP experts and HP experts as ne_1 and ne_2 , respectively. For simplicity, we make them identical in the experiments, denoted as ne . We refer to the number of layers each expert attends to as attention granularity. As the value of ne increases, the attention granularity becomes finer. As shown in Fig. 5, the results from the VTAB-1K benchmark indicate different patterns. For instance, on the DTD dataset, the best performance is achieved when ne is 4, while on sNORB-Azim, performance increases with the increase in ne . Increasing ne leads to more parameters and finer attention granularity. However, finer attention granularity does not necessarily lead to better overall performance. For example, on Resisc45, DTD, Cifar100, sNORB-Ele, dsPr-LoC, Flowers102, and EuroSAT, the negative impact of increasingly finer attention granularity eventually outweighs the benefits of increased parameters, leading to a decrease in overall performance. In other tasks, different patterns may occur because the positive effect of attention granularity on performance is consistently strong, or its negative effect is not enough to offset the benefits of increased parameters, resulting in a generally increasing performance with ne . This phenomenon provides an important insight: for most tasks, simply increasing parameters may not lead to better performance. Instead, only when attention granularity and the number of parameters reach a good tradeoff can we achieve the best performance.

Does Lily Exhibit Selectivity? Lily uses routers to assign varying weights to different HP experts, thereby achieving selective information combination. We illustrate this selectivity in Fig. 6. We use a setup with three HP experts and select three layer levels (1, 13, 22) to calculate the total weight assigned to each expert. The results reveal a clear selectivity: for different layers, the router assigns significantly different weights to different HP experts. For instance, on Cifar100, the middle layer is predominantly dominated by HP 2, whereas the deep layer is primarily dominated by HP 1 and HP 2. In contrast, on Retinopathy, both the middle and deep layers are dominated by HP 3. This selectivity ensures that, even when different layers share information, the inherent differences between layers are still taken into account, making the adaptation more flexible and comprehensive.

5 Conclusion

In this paper, we propose low-rank interconnected adaptation (Lily), a novel framework for efficient fine-tuning via inter-connectivity of adapters. Lily enables each layer to access information from others during adaptation through a hierarchical structure. Additionally, it successfully overcome the low-rank update limitation of LoRA, enabling high-rank update and therefore better adaptation capability. Our approach consistently improves performance across various modalities, model sizes, and architectures, surpassing existing methods with enhanced efficiency. In summary, Lily’s versatility and efficiency make it a promising approach for a wide range of applications.

References

- AI@Meta. Llama 3 model card. 2024. URL https://github.com/meta-llama/llama3/blob/main/MODEL_CARD.md.
- Amjad Almahairi, Nicolas Ballas, Tim Cooijmans, Yin Zheng, Hugo Larochelle, and Aaron Courville. Dynamic capacity networks. In *International Conference on Machine Learning*, pages 2549–2558. PMLR, 2016.
- Yoshua Bengio, Nicholas Léonard, and Aaron Courville. Estimating or propagating gradients through stochastic neurons for conditional computation. *arXiv preprint arXiv:1308.3432*, 2013.
- Dan Biderman, Jose Gonzalez Ortiz, Jacob Portes, Mansheej Paul, Philip Greengard, Connor Jennings, Daniel King, Sam Havens, Vitaliy Chiley, Jonathan Frankle, et al. Lora learns less and forgets less. *arXiv preprint arXiv:2405.09673*, 2024.
- Yonatan Bisk, Rowan Zellers, Jianfeng Gao, Yejin Choi, et al. Piqa: Reasoning about physical commonsense in natural language. In *Proceedings of the AAAI conference on artificial intelligence*, volume 34, pages 7432–7439, 2020.
- Shoufa Chen, Chongjian Ge, Zhan Tong, Jiangliu Wang, Yibing Song, Jue Wang, and Ping Luo. Adaptformer: Adapting vision transformers for scalable visual recognition. *Advances in Neural Information Processing Systems*, 35:16664–16678, 2022.
- Christopher Clark, Kenton Lee, Ming-Wei Chang, Tom Kwiatkowski, Michael Collins, and Kristina Toutanova. BoolQ: Exploring the surprising difficulty of natural yes/no questions. In Jill Burstein, Christy Doran, and Thamar Solorio, editors, *Proceedings of the 2019 Conference of the North American Chapter of the Association for Computational Linguistics: Human Language Technologies, Volume 1 (Long and Short Papers)*, pages 2924–2936, Minneapolis, Minnesota, June 2019.
- Peter Clark, Isaac Cowhey, Oren Etzioni, Tushar Khot, Ashish Sabharwal, Carissa Schoenick, and Oyvind Tafjord. Think you have solved question answering? try arc, the ai2 reasoning challenge. *arXiv preprint arXiv:1803.05457*, 2018.
- Andrew Davis and Itamar Arel. Low-rank approximations for conditional feedforward computation in deep neural networks. *arXiv preprint arXiv:1312.4461*, 2013.
- Jia Deng, Wei Dong, Richard Socher, Li-Jia Li, Kai Li, and Li Fei-Fei. Imagenet: A large-scale hierarchical image database. In *2009 IEEE conference on computer vision and pattern recognition*, pages 248–255. Ieee, 2009.
- Alexey Dosovitskiy, Lucas Beyer, Alexander Kolesnikov, Dirk Weissenborn, Xiaohua Zhai, Thomas Unterthiner, Mostafa Dehghani, Matthias Minderer, Georg Heigold, Sylvain Gelly, et al. An image is worth 16x16 words: Transformers for image recognition at scale. *arXiv preprint arXiv:2010.11929*, 2020.
- David Eigen, Marc’Aurelio Ranzato, and Ilya Sutskever. Learning factored representations in a deep mixture of experts. *arXiv preprint arXiv:1312.4314*, 2013.
- Chongyang Gao, Kezhen Chen, Jinmeng Rao, Baochen Sun, Ruibo Liu, Daiyi Peng, Yawen Zhang, Xiaoyuan Guo, Jie Yang, and VS Subrahmanian. Higher layers need more lora experts. *arXiv preprint arXiv:2402.08562*, 2024a.
- Ziqi Gao, Qichao Wang, Aochuan Chen, Zijing Liu, Bingzhe Wu, Liang Chen, and Jia Li. Parameter-efficient fine-tuning with discrete fourier transform. *arXiv preprint arXiv:2405.03003*, 2024b.
- Albert Gu and Tri Dao. Mamba: Linear-time sequence modeling with selective state spaces. *arXiv preprint arXiv:2312.00752*, 2023.
- Yongchang Hao, Yanshuai Cao, and Lili Mou. Flora: Low-rank adapters are secretly gradient compressors. *arXiv preprint arXiv:2402.03293*, 2024.
- Neil Houlsby, Andrei Giurgiu, Stanislaw Jastrzebski, Bruna Morrone, Quentin De Laroussilhe, Andrea Gesmundo, Mona Attariyan, and Sylvain Gelly. Parameter-efficient transfer learning for nlp. In *International Conference on Machine Learning*, pages 2790–2799. PMLR, 2019a.
- Neil Houlsby, Andrei Giurgiu, Stanislaw Jastrzebski, Bruna Morrone, Quentin De Laroussilhe, Andrea Gesmundo, Mona Attariyan, and Sylvain Gelly. Parameter-efficient transfer learning for nlp. In *International conference on machine learning*, pages 2790–2799. PMLR, 2019b.
- Edward J Hu, Yelong Shen, Phillip Wallis, Zeyuan Allen-Zhu, Yanzhi Li, Shean Wang, Lu Wang, and Weizhu Chen. Lora: Low-rank adaptation of large language models. *arXiv preprint arXiv:2106.09685*, 2021.
- Zhiqiang Hu, Lei Wang, Yihuai Lan, Wanyu Xu, Ee-Peng Lim, Lidong Bing, Xing Xu, Soujanya Poria, and Roy Lee. LLM-adapters: An adapter family for parameter-efficient fine-tuning of large language models. In Houda Bouamor, Juan Pino, and Kalika Bali, editors, *Proceedings of the 2023 Conference on Empirical Methods in Natural Language Processing*, pages 5254–5276, Singapore, December 2023. Association for Computational Linguistics. doi: 10.18653/v1/2023.emnlp-main.319. URL <https://aclanthology.org/2023.emnlp-main.319>.

- Ting Jiang, Shaohan Huang, Shengyue Luo, Zihan Zhang, Haizhen Huang, Furu Wei, Weiwei Deng, Feng Sun, Qi Zhang, Deqing Wang, et al. Mora: High-rank updating for parameter-efficient fine-tuning. *arXiv preprint arXiv:2405.12130*, 2024.
- Shibo Jie and Zhi-Hong Deng. Fact: Factor-tuning for lightweight adaptation on vision transformer. In *Proceedings of the AAAI Conference on Artificial Intelligence*, volume 37, pages 1060–1068, 2023.
- Shibo Jie, Haoqing Wang, and Zhi-Hong Deng. Revisiting the parameter efficiency of adapters from the perspective of precision redundancy. In *Proceedings of the IEEE/CVF International Conference on Computer Vision*, pages 17217–17226, 2023.
- Zhaojiang Lin, Andrea Madotto, and Pascale Fung. Exploring versatile generative language model via parameter-efficient transfer learning. *arXiv preprint arXiv:2004.03829*, 2020.
- Shih-Yang Liu, Chien-Yi Wang, Hongxu Yin, Pavlo Molchanov, Yu-Chiang Frank Wang, Kwang-Ting Cheng, and Min-Hung Chen. Dora: Weight-decomposed low-rank adaptation. *arXiv preprint arXiv:2402.09353*, 2024.
- Yinhan Liu, Myle Ott, Naman Goyal, Jingfei Du, Mandar Joshi, Danqi Chen, Omer Levy, Mike Lewis, Luke Zettlemoyer, and Veselin Stoyanov. Roberta: A robustly optimized bert pretraining approach. *arXiv preprint arXiv:1907.11692*, 2019.
- Sourab Mangrulkar, Sylvain Gugger, Lysandre Debut, Younes Belkada, Sayak Paul, and Benjamin Bossan. Peft: State-of-the-art parameter-efficient fine-tuning methods. <https://github.com/huggingface/peft>, 2022.
- Fanxu Meng, Zhaohui Wang, and Muhan Zhang. Pissa: Principal singular values and singular vectors adaptation of large language models. *arXiv preprint arXiv:2404.02948*, 2024.
- Todor Mihaylov, Peter Clark, Tushar Khot, and Ashish Sabharwal. Can a suit of armor conduct electricity? a new dataset for open book question answering. *arXiv preprint arXiv:1809.02789*, 2018.
- Roy Miles, Pradyumna Reddy, Ismail Elezi, and Jiankang Deng. Velora: Memory efficient training using rank-1 sub-token projections. *arXiv preprint arXiv:2405.17991*, 2024.
- Jonas Pfeiffer, Aishwarya Kamath, Andreas Rücklé, Kyunghyun Cho, and Iryna Gurevych. Adapterfusion: Non-destructive task composition for transfer learning. *arXiv preprint arXiv:2005.00247*, 2020a.
- Jonas Pfeiffer, Aishwarya Kamath, Andreas Rücklé, Kyunghyun Cho, and Iryna Gurevych. Adapterfusion: Non-destructive task composition for transfer learning. *arXiv preprint arXiv:2005.00247*, 2020b.
- Andreas Rücklé, Gregor Geigle, Max Glockner, Tilman Beck, Jonas Pfeiffer, Nils Reimers, and Iryna Gurevych. Adapterdrop: On the efficiency of adapters in transformers. *arXiv preprint arXiv:2010.11918*, 2020.
- Nataniel Ruiz, Yuanzhen Li, Varun Jampani, Yael Pritch, Michael Rubinstein, and Kfir Aberman. Dreambooth: Fine tuning text-to-image diffusion models for subject-driven generation. In *IEEE/CVF Conference on Computer Vision and Pattern Recognition, CVPR 2023, Vancouver, BC, Canada, June 17-24, 2023*, pages 22500–22510. IEEE, 2023. doi: 10.1109/CVPR52729.2023.02155. URL <https://doi.org/10.1109/CVPR52729.2023.02155>.
- Keisuke Sakaguchi, Ronan Le Bras, Chandra Bhagavatula, and Yejin Choi. Winogrande: An adversarial winograd schema challenge at scale. *Communications of the ACM*, 64(9):99–106, 2021.
- Maarten Sap, Hannah Rashkin, Derek Chen, Ronan Le Bras, and Yejin Choi. Social IQa: Commonsense reasoning about social interactions. In Kentaro Inui, Jing Jiang, Vincent Ng, and Xiaojun Wan, editors, *Proceedings of the 2019 Conference on Empirical Methods in Natural Language Processing and the 9th International Joint Conference on Natural Language Processing (EMNLP-IJCNLP)*, pages 4463–4473, Hong Kong, China, November 2019. Association for Computational Linguistics. doi: 10.18653/v1/D19-1454. URL <https://aclanthology.org/D19-1454>.
- Noam Shazeer, Azalia Mirhoseini, Krzysztof Maziarz, Andy Davis, Quoc Le, Geoffrey Hinton, and Jeff Dean. Outrageously large neural networks: The sparsely-gated mixture-of-experts layer. *arXiv preprint arXiv:1701.06538*, 2017.
- Cheng-Hao Tu, Zheda Mai, and Wei-Lun Chao. Visual query tuning: Towards effective usage of intermediate representations for parameter and memory efficient transfer learning. In *Proceedings of the IEEE/CVF Conference on Computer Vision and Pattern Recognition*, pages 7725–7735, 2023a.
- Cheng-Hao Tu, Zheda Mai, and Wei-Lun Chao. Visual query tuning: Towards effective usage of intermediate representations for parameter and memory efficient transfer learning. In *Proceedings of the IEEE/CVF Conference on Computer Vision and Pattern Recognition*, pages 7725–7735, 2023b.
- Mojtaba Valipour, Mehdi Rezagholizadeh, Ivan Kobzyev, and Ali Ghodsi. Dylora: Parameter efficient tuning of pre-trained models using dynamic search-free low-rank adaptation. *arXiv preprint arXiv:2210.07558*, 2022.
- Ashish Vaswani, Noam Shazeer, Niki Parmar, Jakob Uszkoreit, Llion Jones, Aidan N Gomez, Łukasz Kaiser, and Illia Polosukhin. Attention is all you need. *Advances in neural information processing systems*, 30, 2017a.

- Ashish Vaswani, Noam Shazeer, Niki Parmar, Jakob Uszkoreit, Llion Jones, Aidan N Gomez, Łukasz Kaiser, and Illia Polosukhin. Attention is all you need. *Advances in neural information processing systems*, 30, 2017b.
- Alex Wang, Amanpreet Singh, Julian Michael, Felix Hill, Omer Levy, and Samuel R Bowman. Glue: A multi-task benchmark and analysis platform for natural language understanding. *arXiv preprint arXiv:1804.07461*, 2018.
- Hanqing Wang, Zeguan Xiao, Yixia Li, Shuo Wang, Guanhua Chen, and Yun Chen. Milora: Harnessing minor singular components for parameter-efficient llm finetuning. *arXiv preprint arXiv:2406.09044*, 2024.
- Taiqiang Wu, Jiahao Wang, Zhe Zhao, and Ngai Wong. Mixture-of-subspaces in low-rank adaptation. 2024. URL arxiv.org/abs/2406.11909.
- Ted Zadori, Ahmet Üstün, Arash Ahmadian, Beyza Ermiş, Acyr Locatelli, and Sara Hooker. Pushing mixture of experts to the limit: Extremely parameter efficient moe for instruction tuning. *arXiv preprint arXiv:2309.05444*, 2023.
- Elad Ben Zaken, Shauli Ravfogel, and Yoav Goldberg. Bitfit: Simple parameter-efficient fine-tuning for transformer-based masked language-models. *arXiv preprint arXiv:2106.10199*, 2021.
- Rowan Zellers, Ari Holtzman, Yonatan Bisk, Ali Farhadi, and Yejin Choi. Hellaswag: Can a machine really finish your sentence? *arXiv preprint arXiv:1905.07830*, 2019.
- Xiaohua Zhai, Joan Puigcerver, Alexander Kolesnikov, Pierre Ruysen, Carlos Riquelme, Mario Lucic, Josip Djolonga, Andre Susano Pinto, Maxim Neumann, Alexey Dosovitskiy, et al. The visual task adaptation benchmark. 2019.
- Qingru Zhang, Minshuo Chen, Alexander Bukharin, Pengcheng He, Yu Cheng, Weizhu Chen, and Tuo Zhao. Adaptive budget allocation for parameter-efficient fine-tuning. In *International Conference on Learning Representations*. Openreview, 2023.
- Zihan Zhong, Zhiqiang Tang, Tong He, Haoyang Fang, and Chun Yuan. Convolution meets lora: Parameter efficient finetuning for segment anything model. *arXiv preprint arXiv:2401.17868*, 2024.
- Lianghui Zhu, Bencheng Liao, Qian Zhang, Xinlong Wang, Wenyu Liu, and Xinggang Wang. Vision mamba: Efficient visual representation learning with bidirectional state space model. *arXiv preprint arXiv:2401.09417*, 2024.
- Jingwei Zuo, Maksim Velikanov, Dhia Eddine Rhaïem, Ilyas Chahed, Younes Belkada, Guillaume Kunsch, and Hakim Hacid. Falcon mamba: The first competitive attention-free 7b language model. 2024.

Appendix

A More discussion about Lily

A.1 Model Structure and Design Intuition of Lily

Within the overall framework of Lily, we delve into specific implementation details and model design insights. First, we have established the relationship between LPs and HP: LP is confined to specific levels of layers, capturing features that enable the router to selectively assign weights to the HP experts. In contrast, HP is a model-wide module comprising multiple experts, each of which contains information from a particular level of layers. We highlight several key aspects which are not heavily discussed in the methodology section:

A.1.1 Number of LPs

Since LP is limited to specific layers, the simplest approach would be to place an LP at each layer of the module to be adapted (e.g., the query transformation in MHSA). However, this setup may not be necessary: the importance of each layer varies, and many layers have significantly lower importance than others [Zhang et al., 2023]. To achieve greater parameter efficiency, we can set up fewer LPs, with each LP focusing on a level of layers rather than a single layer. For example, an LP can focus on shallow layers (e.g., layers 0, 1, 2, etc.) or deep layers. To enable a single LP to handle multiple layers, we can share an LP across multiple layers. By doing so, we eliminate the redundancy of having an LP at each layer, reduce the number of parameters, and increase efficiency. **This is exactly the strategy adopted by most of the experiments.**

A.1.2 Number of HP Experts

Regarding HP, the number of experts can be arbitrarily set, enabling more flexible configurations. In our experiments, for the sake of simplicity, we set the number of HP experts equal to the number of LPs, thereby equating the granularity of LP and HP.

A.1.3 Routers Setup

There are also different settings that can be employed for the router. First, we can bind the router to HP, resulting in only one router per model. However, since the number of parameters in the router is relatively small, having only one router per model may not lead to significant selectivity. Therefore, we can also bind the router to LP, configuring a separate router for each LP. Most of our experiments use the latter setup, but in the vision experiments on Vim, we use the single-router and no-lp-sharing setup to verify its effectiveness. From the results, we can see that this setup also performs well. As future work, we can verify the effectiveness of using the latter setup on Vim, which may potentially lead to superior performance.

A.1.4 Hyperparameters

We detail the hyperparameters used in Lily. Specifically, we use **lily_r** to represent the hidden-dimension of the projectors: LPs and HPs. It serves the same function as **r** in LoRA. We use **lily_s** to represent the scaling factor used by Lily. It is mostly searched within the range of {0.01, 0.1, 1.0, 10.0, 100.0}. We use **ne_1** to represent the number of LPs used in the model. Since the LPs can be shared as discussed in the previous section, **ne_1** does not need to equal the number of layers in the model. We use **ne_2** to represent the number of HP experts in the model-wide HP module. In our experiments, we set **ne_1 = ne_2** to improve parameter-efficiency and simplicity.

A.1.5 Design Intuition

Lily employs a hierarchical structure to enable updates with higher-ranks than LoRA. However, simply equally connecting all the HPs to the LPs can not achieve the best performance. From the perspective of feature and information utilization across layers, simply aggregating all HPs for an LP ignores the distinctness of the features from current layers. Meanwhile, it reduced the variability of the combinations of gradient projection matrices (S_i and $C_{i,j}$ are constants now), making the rank of the weight update higher than that of LoRA (since multiple distinct random matrices are used), but still not high enough for the best performance because of the lack of variability during combination. Therefore, we introduce selectivity into the inter-connectivity as well as discussed below, making the combination of HPs data-dependent so that each S_i is unique across the time-steps, enabling updates with even higher ranks. The approach has similarity to Hao et al. [2024], where random matrix is constantly resampled to ensure updates with higher ranks. We further conduct an analysis in Appendix G.

```

1  class lily_adapter(nn.Module):
2      """
3      Implementation of a Lily adapter for an adaptation target.
4
5      Args:
6          in_dim: input dimension
7          out_dim: output dimension
8          hidden_dim: hidden dimension
9          ne: number of experts
10         lp: low-dimensionl projector
11         hps: high-dimensionl projector experts
12         mlp: whether the adpatation target is located in MLP
13     """
14     def __init__(self, hidden_dim, ne, lp, hps, mlp=False):
15         super().__init__()
16         self.hps = hps
17         self.ne = ne
18         self.lp = lp
19         self.router = nn.Linear(hidden_dim, ne, bias=False)
20         if mlp:
21             self.non_linear = nn.ReLU()
22         else:
23             self.non_linear = nn.Identity()
24     def forward(self, x):
25         hidden = self.non_linear(self.lp(x))
26         router_logits = self.router(hidden) # [B, N, num_of_experts]
27         router_probability = F.softmax(router_logits, dim=-1) # [B, N, ne]
28         expert_probabilities = router_probability.mean(dim=(0, 1))
29         combined_hp = torch.einsum("e,eio->io", expert_probabilities, self.hps)
30         return torch.matmul(hidden, combined_hp)

```

Figure 7: Implementation of Lily in VTAB-1K benchmark.

A.2 Efficient Implementation for Weighted Combination

One intuitive implementation of the weighted combination in Lily is Eq. 17, from which we could observe that it perform N_e times of matrix multiplication, N_e times of scalar multiplication and N_e times of matrix addition. Therefore, despite its intuitive nature, the computational burden of this approach is quite formidable.

However, Eq. 18 which is adopted in Lily only utilize N_e times of scalar multiplication, N_e times of matrix addition and 1 time of matrix multiplication. This saves roughly N_e times of matrix multiplication, which can be significant as the size of the model and number of adaptation targets increases. For a x' size of $\mathbb{R}^{N \times d}$ and a $P_H \in \mathbb{R}^{d \times C}$, the floating-point operation (FLOPs) of these two implementation are:

$$\begin{aligned}
 \text{FLOPs} &= \sum_1^{N_e} (2NdC) + \sum_1^{N_e} (dC) + \sum_1^{N_e} (NC) \\
 &= N_e \times (2NdC + dC + NC) \quad (\text{Intuitive}) \\
 \text{FLOPs} &= 2 \sum_{i=1}^{N_e} (dC) + 2NdC \\
 &= 2dC \times (N + N_e) \quad (\text{Lily})
 \end{aligned} \tag{21}$$

from which we can easily observe that the approach adopted by Lily requires less computation and therefore provides more speed and efficiency during the fine-tuning process. Under the setting of $N = 1024, d = 16, C = 768, N_e = 4$, the FLOPs of the intuitive approach would be 0.104 GFLOPs while in Lily it is merely 0.025 GFLOPs, which could potentially lead to a 4X increase in speed.

A.3 Actual implementation of Lily

We present the actual implementation of Lily in Fig. 7. For the example here, we choose the implementation from visual adaptation tasks (i.e., VTAB-1K benchmark). For LLM, the implementation is a bit more complicated because

of modifications to the huggingface PEFT library [Mangrulkar et al., 2022], but the fundamental adaptation process is the same. Specifically, given an input, we first use the corresponding LP of the current layer to project it to a low-dimensional representation. After that, we use the low-dimensional representation to selectively assign weights for the HP experts. Once we obtain all the weights for the experts, we set out to combine these HP experts accordingly, as discussed in Appendix A.2. After the weighted combination, we use the obtained combined HP to project the low-dimensional representation to high-dimension, therefore acquiring the extra knowledge gained through adaptation.

B Experimental settings

B.1 Hyper-parameters

A detailed description of the hyper-parameters used in Lily is in Appendix A.1.

B.1.1 Commonsense Reasoning

The hyper-parameters used in commonsense reasoning experiments for MiLoRA, PiSSA are provided in Table 7, 6. Settings for Lily and LoRA using Falcon-Mamba as the backbone are provided in Table. 9 and 8. It can be noticed that Lily achieves the best performance by merely adapting the multi-head self attention module (MHSA) in LLaMA3-8B, while other compared methods adapt all the modules including MLP. Meanwhile, Lily employs the least amount of parameters, showcasing its excellent adaptation at low parameter-budget scenarios.

Table 6: Hyperparameter configuration from the MiLoRA paper.

MiLoRA hyperparameters	
Rank r	32
α of LoRA	64
α of PiSSA	32
Dropout	0.05
Optimizer	AdamW
LR	$3e-4$
LR Scheduler	Linear
Batch Size	16
Warmup Steps	100
Epochs	3
Placement	query, key, value, MLP up, MLP down

Table 7: Hyperparameter configuration from the PiSSA paper.

PiSSA hyperparameters	
α	Same as rank r
Dropout	0.0
Optimizer	AdamW
LR	$2e-5$
LR Scheduler	cosine
Batch Size	128
Warmup Ratio	0.03
Epochs	1
Placement	query, key, value, output, gate, MLP up, MLP down

B.1.2 Natural Language Understanding

Specific hyper-parameter settings of Lily on GLUE benchmark are provided in Table 10. We fix the learning rate of both the backbone and the head as $5E-3$ and tune the scaling factor $\text{lily_s} \in \{0.01, 0.1, 1.0\}$ instead. For the rank r we fix it to 32 and the seed to 0.

Table 8: Hyperparameter configuration for LoRA using Falcon-Mamba as backbone.

LoRA hyperparameters	
Rank r	2
α	16
Dropout	0.05
Optimizer	AdamW
LR	3e-4
LR Scheduler	Linear
Batch Size	16
Epochs	1
Placement	input, delta

Table 9: Best Hyperparameter configuration for Lily using Falcon-Mamba and LLaMA3 as backbones.

	Falcon-Mamba	LLaMA3
Rank r	40	16
ne_1	4	4
ne_2	4	4
Dropout	0	0
Optimizer	AdamW	AdamW
LR	3e-4	3e-4
LR Scheduler	Linear	Linear
Batch Size	16	16
Epochs	1	3
Placement	input	query, key, value

B.1.3 Visual Adaptation Benchmark

We provide the hyper-parameter for Lily on VTAB-1K benchmark in Table 11. Specifically, we fix the learning rate at $1E-3$ with a weight decay of $1E-4$. For ViT, we tune the scaling factor $lily_s \in \{0.01, 0.1, 1.0, 10.0\}$ to maximize the performance, following Jie et al. [2023], Jie and Deng [2023]. For Vim, we fix $lily_s$ to 1.0. Additionally, we search for the hyper-parameters ne_1 and ne_2 within the range $\{2, 3, 4\}$, as these numbers can divide the number of layers in the ViT model (12 in ViT-B). For vim, we use the implementation discussed in section A.1, which does not share LPs across layers. Therefore, ne_1 in this setting is fixed to number of layers in Vim (22 in this case), while we search ne_2 in $\{3, 6\}$ and $\{5, 6, 17\}$ separately for Lily-S and Lily-L. Note that ne is only set for input projection in Vim. For delta transformation, we only use a single HP expert to reduce the parameter cost. In the experiments of ViT, the rank r is fixed at 16. Meanwhile in Vim’s setting, we tune the ranks r for the delta transformation module and the input projection module separately. We use 4, 4 and 4, 8 separately for Lily-S and Lily-L.

B.2 Datasets

B.2.1 Commonsense Reasoning

We provide a short description of each datasets used in commonsense reasoning experiments in Table 12.

B.2.2 Natural Language Understanding

We provide detailed information about datasets in the GLUE benchmark in Table 13.

B.2.3 Visual Adaptation Benchmark

We provide detailed information about all the tasks from VTAB-1K benchmark in Table 14.

Table 10: Hyperparameter of Lily on GLUE benchmark.

Hyperparameter	STS-B	RTE	MRPC	CoLA	SST-2	QNLI	MNLI	QQP
Optimizer	AdamW							
LR Schedule	Linear							
Learning Rate (Lily)	5e-3							
Learning Rate (Head)	5e-3							
Max Seq. Len	512	512	512	512	512	512	512	512
Lily_s	0.1	0.1	0.1	0.01	0.01	0.01	0	0
ne_1	2	3	2	4	2	2	0	0
ne_2	2	3	2	4	2	2	0	0
Batch Size	64	32	50	64	32	32	0	0

Table 11: Hyperparameter configuration for Lily on VTAB-1K benchmark.

	Vision Transformer	Vision Mamba
Optimizer	AdamW	AdamW
Batch Size	64	64
Learning Rate	1E-3	1E-2
Weight Decay	1E-4	1E-3
# Epochs	100	100
LR Decay	cosine	cosine

Table 12: Details of the datasets used in our commonsense reasoning tasks.

Benchmark	Description	# Test Questions
ARC-c	Multiple-choice science	2376
ARC-e	Multiple-choice science	1172
OBQA	Multi-step reasoning	500
SIQA	Social implications	1954
WinoG	Fill-in-a-blank	1267
PIQA	Physical commonsense	1830
BoolQ	Yes/no questions	3270
HellaS	Commonsense NLI	10042

C Does Sharing LP Results in Inferior Performance?

As mentioned earlier, we adopted a strategy of sharing the LP across most of our experiments, ensuring that the number of LP and HP experts is consistent. This approach offers two benefits: simplicity and enhanced parameter efficiency. By sharing the LP, we eliminate the need to set a separate LP for each layer, thereby reducing the overall parameter count.

Our decision to share the LP is based on the observation of overall redundancy among layers. Specifically, different layers have varying levels of importance [Zhang et al., 2023], and some less important layers do not require a dedicated LP. By not setting a separate LP for these layers, we avoid introducing extra parameter overhead while having a negligible impact on performance. To test that whether sharing LP results in inferior performance, we conduct experiments with no LP sharing on VTAB-1K. The results are shown in Table 15, from which we can observe that the best overall performance (77.3%) is the same as that in the LP-sharing setting. This indicates that even if we employ one LP for each layer, the performance gain is negligible and many of the parameters are actually redundant. However, not sharing LPs results in extra parameter overhead and damages the parameter-efficiency of Lily. Therefore, LP-sharing is a great strategy to eliminate redundancy among LPs and boost the parameter-efficiency of Lily.

Table 13: Information about datasets in the GLUE benchmark, with STS-B being a regression task and all other tasks falling into the categories of single-sentence or sentence-pair classification.

Corpus	Metrics	Task	# Train	# Val	# Test	# Labels
Single-Sentence Tasks						
CoLA	Matthews Corr.	Acceptability	8.55k	1.04k	1.06k	2
SST-2	Accuracy	Sentiment	67.3k	872	1.82k	2
Similarity and Paraphrase Tasks						
MRPC	Accuracy/F1	Paraphrase	3.67k	408	1.73k	2
STS-B	Pearson/Spearman Corr.	Sentence similarity	5.75k	1.5k	1.38k	1
QQP	Accuracy/F1	Paraphrase	364k	40.4k	391k	2
Inference Tasks						
MNLI	Accuracy	NLI	393k	19.65k	19.65k	3
QNLI	Accuracy	QA/NLI	105k	5.46k	5.46k	2
RTE	Accuracy	NLI	2.49k	277	3k	2

Table 14: Detailed information about the datasets in VTAB-1K benchmark.

	Dataset	Train	Val	Test	#Classes
VTAB-1k	CIFAR100			10,000	100
	Caltech101			6,084	102
	DTD			1,880	47
	Oxford-Flowers102			6,149	102
	Oxford-Pets			3,669	37
	SVHN			26,032	10
	Sun397			21,750	397
	Patch Camelyon			32,768	2
	EuroSAT			5,400	10
	Resisc45	800/1,000	200	6,300	45
	Retinopathy			42,670	5
	Clevr/count			15,000	8
	Clevr/distance			15,000	6
	DMLab			22,735	6
	KITTI-Dist			711	4
	dSprites/location			73,728	16
	dSprites/orientation			73,728	16
	SmallNORB/azimuth			12,150	18
	SmallNORB/elevation			12,150	18

D Where to Apply Lily in Transformers?

PEFT methods have been predominantly explored on the Transformer architecture, which consists of multi-head self-attention (MHSA) and multi-layer perceptron (MLP) as its core modules. In this section, we analyze the impact of fine-tuned modules on performance using Lily. Specifically, we compare Lily’s performance on the VTAB-1K benchmark under four settings:

- Applying Lily solely to the query and value transformation module in MHSA (denoted as "qv").
- Applying Lily solely to the MLP module (denoted as "mlp").
- Applying Lily to both the query and value transformation module in MHSA and the MLP module (denoted as "qvmlp").
- Applying Lily to both the key and value transformation module in MHSA and the MLP module (denoted as "kvmlp").

To ensure a fair comparison, we tune the hyperparameters to maintain a similar parameter count across all settings. Additionally, to further investigate whether sharing the low-rank projection (LP) affects performance, we do not share

Table 15: Performance on VTAB-1K benchmark when applying Lily to various modules in Transformer. The implementation here does not share LP for simplicity (i.e., each layer has one LP).

	Average	Natural							Specialized				Structured							
		Cifar100	Caltech101	DTD	Flowers102	Pets	SVHN	Sun397	Camelyon	EuroSAT	Resisc45	Retinopathy	Clevr-Count	Clevr-Dist	DMLab	KITTI-Dist	dSpr-Loc	dSpr-Ori	sNORB-Azim	sNORB-Ele
qv	76.9	73.2	92.3	72.2	99.3	91.4	89.0	56.5	87.6	95.2	84.8	75.9	83.7	65.8	52.8	81.2	87.6	52.4	36.3	43.4
mlp	77.0	74.0	92.6	72.2	99.4	91.5	89.0	55.9	88.2	95.5	85.4	76.0	83.3	63.1	53.0	81.4	86.5	53.8	35.6	43.3
qvmlp	77.1	73.9	93.2	72.7	99.4	91.6	89.7	56.5	87.9	95.3	85.0	76.1	84.6	65.2	53.0	82.1	86.7	53.0	36.0	42.8
kvmlp	77.3	74.0	92.3	72.6	99.3	91.5	89.2	56.7	88.2	95.4	85.3	76.0	84.6	64.9	53.4	81.7	87.5	52.9	36.9	45.2

the LP in this experiment. The results are presented in Table 15. We observe that the "kvmlp" setting achieves the best performance, with an average accuracy of 77.3%. In contrast, adapting only the MHSA module ("qv") yields the worst performance. Furthermore, we note that adapting both the MHSA and MLP modules (qvmlp and kvmlp) generally leads to superior results compared to adapting only one specific module (qv and mlp). This suggests that both MLP and MHSA play crucial roles in the overall model performance, and adapting both is essential for effective adaptation.

Notably, even when applying Lily solely to the MHSA module, which results in the worst performance among the four settings (76.9%), it still outperforms LoRA by a significant margin (0.5%). This underscores the efficiency of Lily, as it uses fewer parameters than LoRA even without LP sharing.

E Where to Apply Lily in Mamba?

Nearly all previous PEFT method studies have been centered around Transformers, while Mamba is a relatively new architecture, so there has been little research on PEFT methods on Mamba. In this section, we briefly analyze the pros and cons of adapting Mamba's modules. In brief, a Mamba block consists of regular linear projection layers and a core component SSM module [Gu and Dao, 2023] [Zhu et al., 2024]. Specifically in SSM module, Mamba utilize parameters (Δ , A , B , C) to transform an input sequence $x(t)$ to an output sequence $y(t)$ using a hidden state $h(t)$. The discretization process converts A and B into \bar{A} and \bar{B} , respectively, using the time step size parameter Δ . Structured state space models, inspired by continuous systems, can be computed similarly to RNNs or in the form of global convolution due to their linear time invariance (LTI) property. Mamba introduces a selective property to structured state space model, tying parameters to the current input, which breaks the LTI property and hinders parallel training. To address this, Mamba employs a hardware-aware algorithm, enabling its SSM module to possess the selective property and perform parallel training. To be specific, the discretization process can be expressed as:

$$\begin{aligned}\bar{A} &= \exp(\Delta A) \\ \bar{B} &= (\Delta A)^{-1}(\exp(\Delta A) - I) \cdot \Delta B\end{aligned}\tag{22}$$

After that, the calculation in Mamba can be expressed as:

$$\begin{aligned}h_t &= \bar{A}h_{t-1} + \bar{B}x_t \\ y_t &= Ch_t\end{aligned}\tag{23}$$

where h_t is the hidden state at time t and x_t is the corresponding input token. Delta projection is a module in SSM that's learnable and tasked with transforming the parameter Δ . Since adapting the delta projection alone can indirectly adapt the entire SSM module (i.e., \bar{A} and \bar{B} are all determined by Δ), it is the most critical component of the SSM module.

We investigate the performance of two adaptation strategies: adapting only the input linear projection layer (denoted as "in") and adapting both the input linear projection layer and SSM (denoted as " Δ + in" since we only adapt delta projection in SSM module). Our results, as shown in Table 1, indicate that applying Lily solely to the input projection yields better performance than applying it to both the input and delta projection modules. This suggests that when adapting Mamba-based models under the paradigm of low-rank adaptation, it is optimal to adapt only the input projection module outside the SSM module. These findings highlight the need for further research into the impact of fine-tuned modules in Mamba on overall performance. Additionally, developing PEFT methods specifically tailored to Mamba-based models, whether for vision or language foundation models, is also a promising direction for future work.

Table 16: Commonsense reasoning results of Lily under various learning rates.

Model	Lr	BoolQ	PIQA	SIQA	HellaSwag	WinoGrande	ARC-e	ARC-c	OBQA	Avg.
LLaMA3-8B	1e-3	70.7	84.6	77.6	87.8	77.3	88.5	74.1	80.8	80.2
	5e-4	71.8	86.5	77.9	82.8	83.1	88.6	76.8	81.4	81.1
	3e-4	72.9	85.6	77.8	92.7	83.3	89.7	77.6	82.8	82.8

```

1 class lily_monoscale(nn.Module):
2     def __init__(self, hidden_dim, ne, lp, hps, mlp=False):
3         super().__init__()
4         self.hps = hps
5         self.ne = ne
6         self.lp = lp
7         self.scale = 1 / ne
8         if mlp:
9             self.non_linear = nn.ReLU()
10        else:
11            self.non_linear = nn.Identity()
12        def forward(self, x):
13            hidden = self.non_linear(self.lp(x))
14            combined_hp = torch.sum(self.hps, 0) * self.scale
15            return torch.matmul(hidden, combined_hp)

```

Figure 8: Implementation of Lily with no selectivity.

F Performance with Different Learning Rates

Since we only tuned the learning rate in the commonsense reasoning experiment, we provide the performance of commonsense reasoning under different learning rates in Table 16.

G Does Selectivity Help?

Lily introduced selective weight combination to selectively incorporate information from other layers. To verify the effectiveness of this selectivity, we remove the router from Lily and evaluate the impact. The modified algorithm without the router is presented in Fig. 8. We conduct experiments on commonsense reasoning to investigate the effect of removing selectivity from Lily.

As shown in Table 17, removing selectivity from Lily results in generally poorer performance compared to vanilla Lily. This is likely because the lack of selectivity causes Lily to simply aggregate all the HP expert, leading to inferior performance. This validates the design choice of using routers in Lily to selectively allocate weights to HP experts, rather than simply summing them.

Table 17: Commonsense reasoning results of Lily without selectivity. We provide results using two learning rates.

Model	Lr	BoolQ	PIQA	SIQA	HellaSwag	WinoGrande	ARC-e	ARC-c	OBQA	Avg.
LLaMA3-8B	3e-4	64.0	82.6	78.5	77.0	79.6	88.4	74.5	82.0	78.3
	5e-4	71.3	85.5	78.1	84.3	79.6	86.4	76.1	79.0	79.8

H How to Allocate Parameters?

Since Lily alters the traditional LoRA’s layer-bound setup, increasing the parameters of Lily can be achieved through two approaches: 1) increasing ne , i.e., increasing the number of LP and HP experts, and 2) increasing the rank, i.e., increasing the parameter size of each individual LP or HP expert. In this section, we investigate which factor has the greatest impact on performance. We conduct experiments on the commonsense reasoning task. Specifically, we maintain the same parameter count and learning rate, and achieve the same parameter count by setting different ranks and adjusting the corresponding ne (e.g., $r=16$, $ne=4$ versus $r=8$, $ne=8$). The results are shown in Fig. 9, from which we observe that more LP and HP experts with smaller rank (i.e., bigger ne and smaller rank) generally performs worse. We

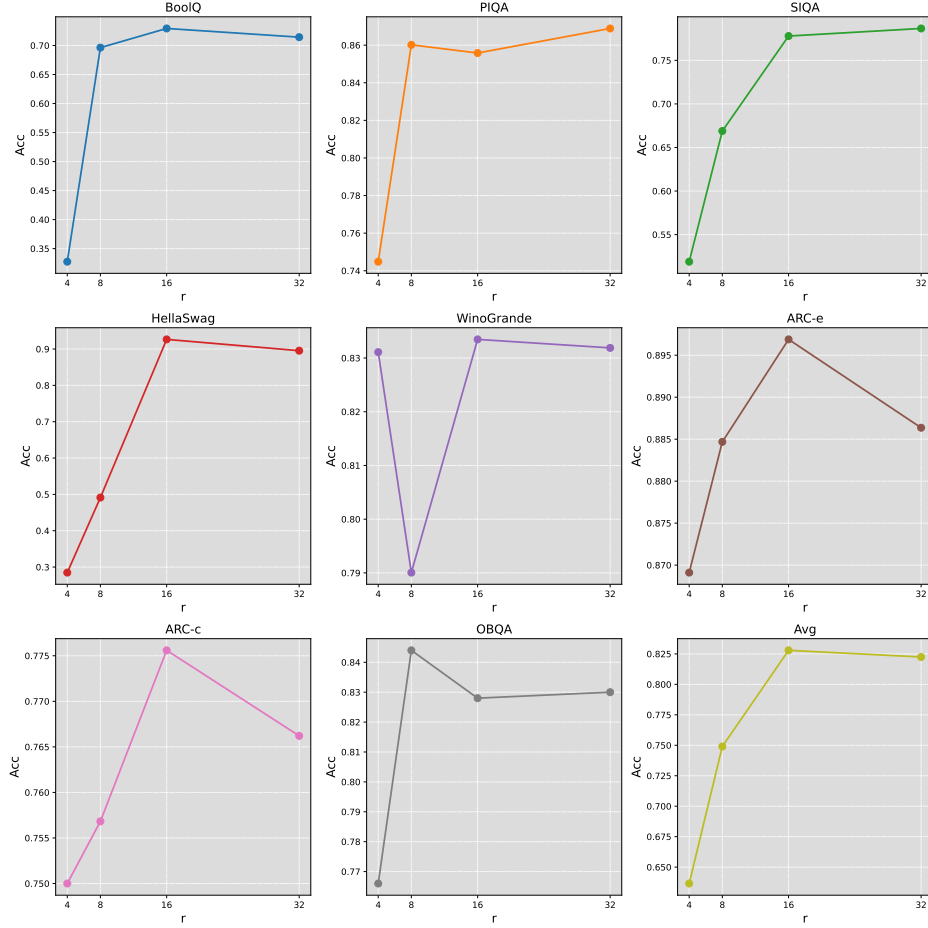


Figure 9: Results on commonsense reasoning tasks when applying different settings of rank. The hyperparameter ne is specifically tuned to maintain the same amount of parameter count for a fair comparison.

argue that this is because, although increasing the attention granularity allows for finer details, the resulting performance gain is not as significant as the gain obtained by increasing the rank, i.e., increasing the model’s capacity to learn more information. This gives us an insight that, in Lily, increasing ne to increase the parameters is less effective than directly increasing the rank in terms of potential performance gain.

I More on Subject-driven Generation

We provide more results on subject-driven generation in Fig. 10 and Fig. 11.

J More on Attention Maps of Lily and LoRA

We provide more visualization results of the attention map from both LoRA and Lily on Caltech101 dataset from VTAB-1K benchmark in Fig. 12.

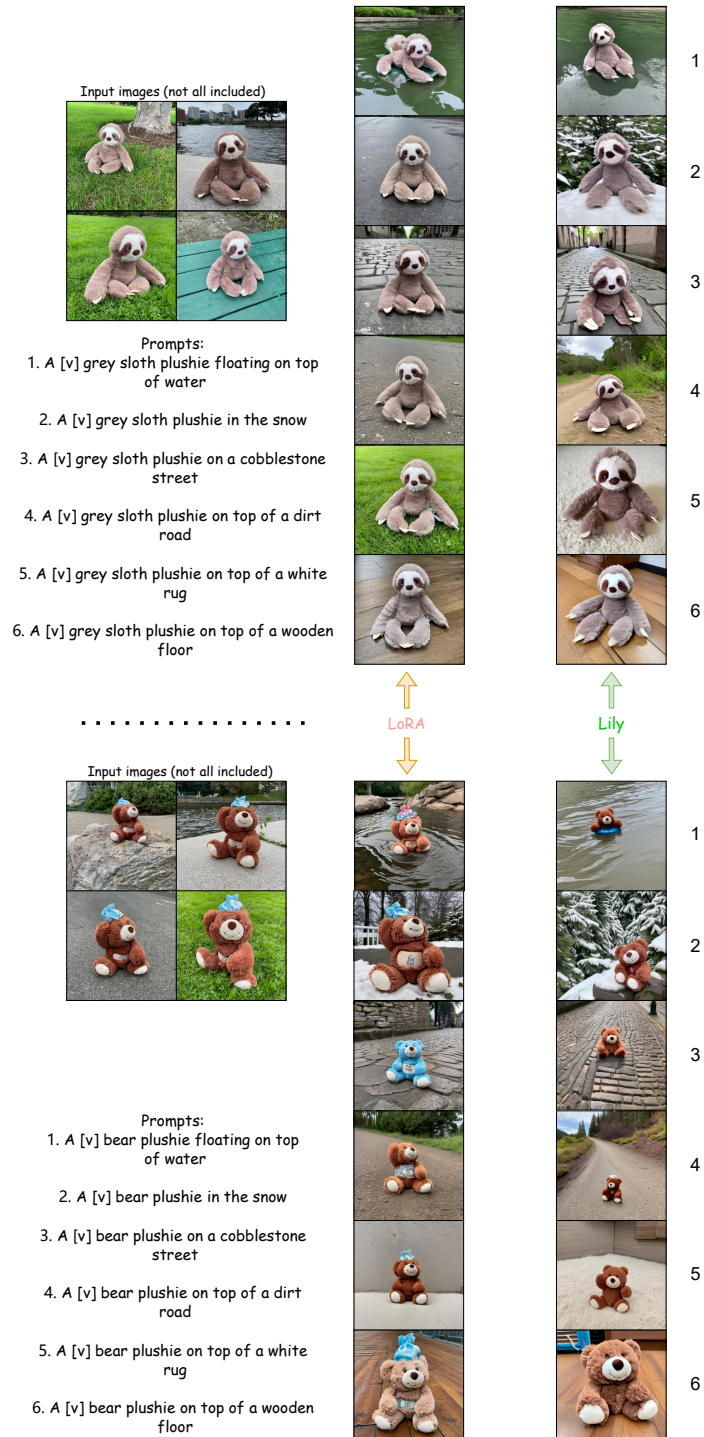


Figure 10: More subject-driven generation results for unreported subjects.

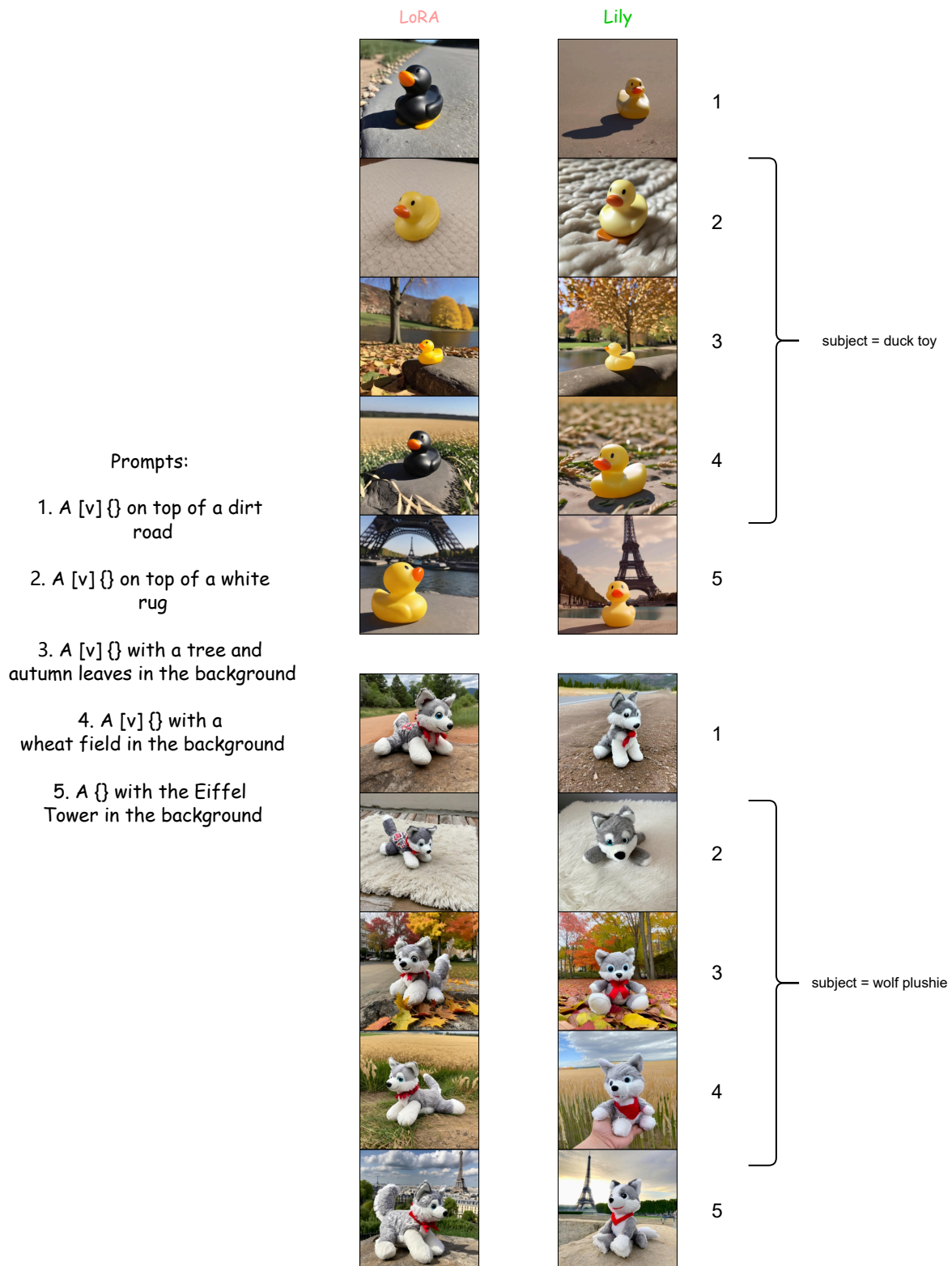


Figure 11: More subject-driven generation results for subjects that are reported in the experiment section.

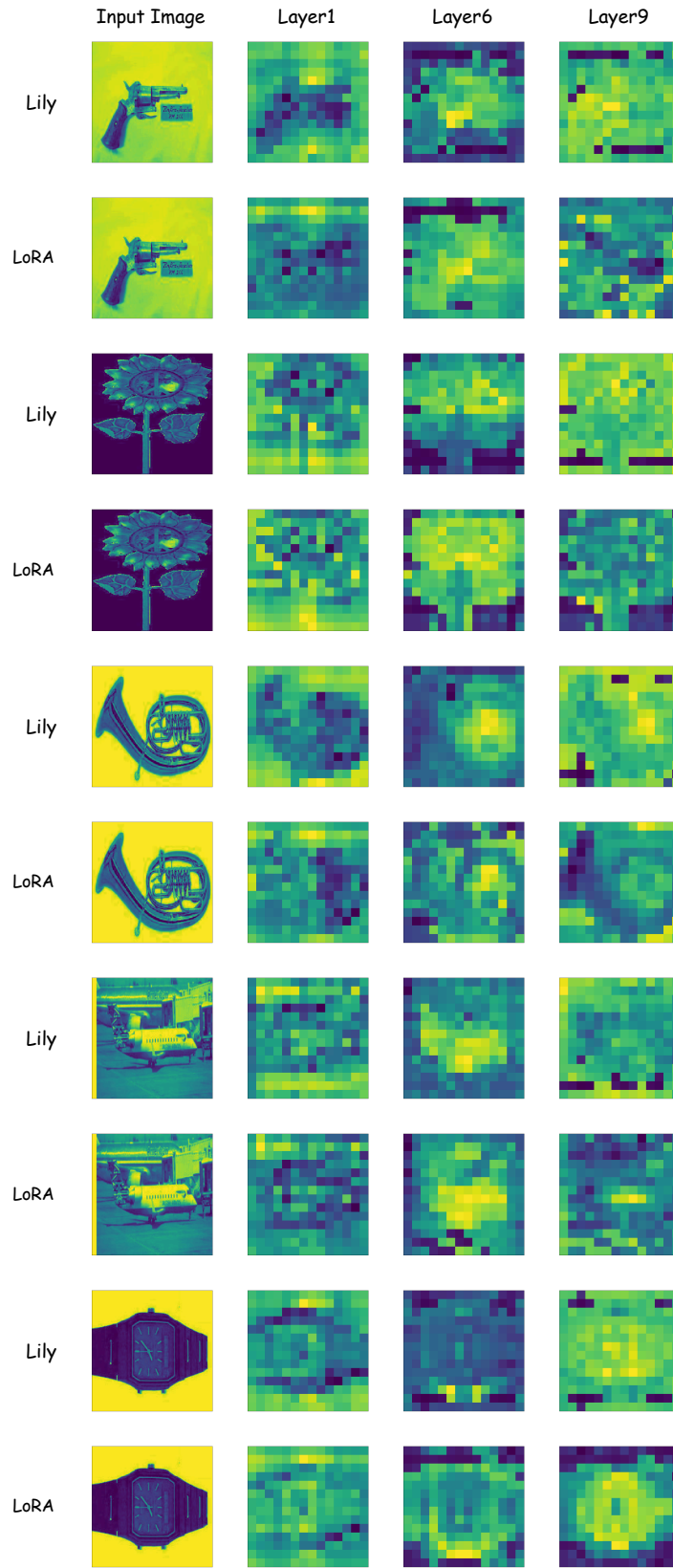


Figure 12: More results of attention maps from LoRA and Lily. All images are taken from Caltech101 dataset.